A Simulation Modeling Framework with Autonomous Vehicle Region-based Routing and Public Transit Diversion Integration

[1]Simon I. Ware, [2]Antonis F. Lentzakis, [3]Rong Su

***Abstract*—In this paper, we present a simulation modeling framework that can accommodate multiple classes of travelers and integrates several distinct features, which in turn can be associated with each of the traveler classes, thus providing flexibility and a so-called bird's-eye view to any potential user. Concretely, we integrate into the multi-class region-based dynamic traffic model, called multi-class Network Transmission Model (McNTM), several features, including a public transit diversion component, as well as routing methods associated with different traveler classes. Three distinct traveler classes are defined, the 1^{st} class of travelers equipped with autonomous vehicles, the 2^{nd} traveler class comprising of RGIS-equipped, conventional vehicles and the 3^{rd} traveler class comprising of unequipped, conventional vehicles. Certain assumptions are made for each traveler class. The gain in overall performance for the case where 1^{st} and 2^{nd} class travelers are present in the system, ranges from 0.78% - 23.43%. Region-based routing methods employed by the 1^{st} and 2^{nd} class respectively, not only benefit overall network performance, but with their respective market penetration rates exceeding certain thresholds, can prove beneficial to the individual performance of other traveler classes.**

Index Terms – autonomous vehicles, public transit, hybrid route choice model, simulation

I. Introduction

The number of autonomous vehicles is projected to rise significantly within the total vehicle population in metropolitan areas. Passenger safety is expected to increase significantly when autonomous vehicles are deployed on urban traffic networks, since human error accounts for 94% of road accidents [1]. This will also cascade into a positive effect on traffic delays given that, currently, 10%-30% of delays can be directly attributed to congestion [2]. Bansal and Kockelman forecast for various combinations of consumers' annual WPT (Willingness To Pay) and technology price drop rates, that by 2045, self-driving vehicles may comprise between 24.8% and 87.2% of the vehicle population in U.S. cities [3]. Modern vehicle navigation systems can provide a plethora of diverse information, which, however, can lead to decision-making behavior that can be hard to anticipate and model accurately. Prescriptive route guidance provides travelers with a single route option, with the implicit guarantee of a shorter travel time. Prescriptive routing, in coordination with traffic operations centers, can lead to system-wide benefits and potential maximization of social welfare. Region-based routing presents a set of region sequences that travelers are encouraged to follow and can help alleviate congestion through near-optimal distribution of vehicles along different regional paths with similar origin and destination locations. Reliable region-based routing information, similarly to link-by-link routing, relies on accurate travel time estimation. This is dependent on accurately evaluating how congested the regions comprising the available regional paths are. To estimate the level of congestion at a regional level, the Network Fundamental Diagram (NFD) is used, which relates vehicle regional vehicle count (accumulation) to length-weighted average network flow (production). Low Network link density variability is instrumental for the derivation of well-defined NFDs, as demonstrated in [4]–[6]. NFDs have been used extensively in research into traffic light control schemes along regional boundaries, [7]–[10], toll pricing schemes [11]–[15], as well as routing applications [16]–[20]. It should be noted that network topology, travel demand distribution, route choice and traffic light settings may affect network production and thus, NFD shape and critical values, [21]–[24]. In order to ameliorate such effects, it is advisable to partition the urban traffic network into homogeneously congested regions which will result in well-defined NFDs, [25]–[27]. The public transit diversion component of our framework can be considered as an additional choice which does not induce travelers to pre-/postpone their departure. This feature could also be amenable for use in a link-based routing approach, assuming the destination location is within walking distance of a station, or when coordination of transportation services occurs, as has recently been the case for public transit operators in the U.S., which have undertaken collaboration initiatives with Lyft and Uber for increased coordination among their respective services [28]. In this paper, we present a simulation modeling framework that can accommodate multiple classes of travelers and integrates several distinct features. These features can be associated with each of the traveler classes, thus providing flexibility and a so-called bird's- eye view to any potential user. Concretely, we integrate into the multi-class region-based dynamic traffic model presented in [20], several features, including a public transit diversion component and routing methods, which are associated with different traveler classes.

The objective of this paper is to demonstrate the application of the proposed framework on a honeycomb network comprising of regular hexagonal regions and to subsequently analyze the individual performance associated with each traveler class, as well as the total network

[1]Simon I. Ware is a Data Scientist with Grab, Singapore simianware@gmail.com

[2]Antonis F. Lentzakis is a Postdoctoral Research Associate with Future Urban Mobility IRG, Singapore-MIT Alliance for Research and Technology, Singapore antonios@smart.mit.edu

[3]Rong Su is Associate Professor with the School of Electrical and Electronic Engineering, Nanyang Technological University, Singapore rsu@ntu.edu.sg

performance. Our test case makes use of scenario 2 from [3] for use in a market penetration scheme, which, based on the current global political climate, constitutes a plausible representation of a moderate progression of autonomous vehicle technology adoption, over a span of 25 years. For convenience, we will refer to scenario 2 as $S2$. For $S2$, it is assumed that all autonomous vehicles are privately owned, with no substantial regulations put in place, to dictate the purchase and use of autonomous vehicles. We have chosen this particular scenario because it is, in our opinion, representative of the current trend in policymaking in the U.S., with the deregulation of autonomous vehicle technology by the federal government as a marked example [29]. We choose to associate autonomous vehicles with the 1^{st} class of travelers which employs predictive routing and are expected to be fully compliant. We associate conventional connected vehicles, equipped with non-predictive RGIS (Route Guidance and Information Systems), with the 2^{nd} traveler class. Travelers that belong to this class, have the option to ignore the routing information prescribed to them. We associate all unequipped human-driven vehicles with the 3^{rd} traveler class. It should be noted that the 2^{nd} traveler class can be split into two subclasses, 2^{nd}_{co} and 2^{nd}_{nc}. The non-compliant subclass 2^{nd}_{nc} will be expected to behave identical with the 3^{rd} class, i.e. in a self-interested manner.

The paper is organized as follows, in Section II, Multi-class Network Transmission Model (McNTM), a region-based dynamic traffic model that employs the NFD concept is briefly described. In Section III, region-based routing methods, both predictive and non-predictive, are presented, used as control inputs to McNTM. These routing methods come integrated with a public transit diversion component, and are associated to traveler classes which employ vehicles of varying technological sophistication. These methods will subsequently be used to represent different traveler classes as described above. In Section IV we present our honeycomb network setup. We also introduce $S2$, an autonomous technology adoption scenario as part of a market penetration scheme. We then use our simulation results to compare the individual performance of each traveler class, as well as the overall network performance. In Section V we present our conclusions and possible future work.

II. Multi-class Network Transmission Model

In order to describe region-based traffic dynamics, we make use of a multi-class extension of the Network Transmission Model, first proposed by Knoop et al. [30]. The McNTM, first introduced in [20], employs the NFD concept to describe the regional traffic dynamics of a network with travel demand comprising of traveler classes with distinct characteristics. Besides taking into consideration the boundary capacity on adjacent regions, McNTM also utilizes origin-/destination-specific accumulations, as well as pre-trip information in the form of regional branching rates.

Let a directed graph $G = (\mathcal{N}, \mathcal{A})$ denote the regional traffic network, which comprises a set of homogeneously congested regions $\mathcal{N}$ and a set of adjacent region boundaries $\mathcal{A} \subseteq \mathcal{N} \times \mathcal{N}$ with boundary capacity matrix $B = \left[b_{i,j}\right]^{|N|\times|N|} \geq 0,\ b_{i,j} > 0 \iff (i,j) \in \mathcal{A}$. We consider a subset of the regions $\mathcal{N}_s \subset \mathcal{N}$ to be the origins and a separate subset $\mathcal{N}_t \subset \mathcal{N}$ to be the destinations. We use

$$Q_i(n_i(h)) = n_i(h) v_{i,f} exp\left(-0.5\left(\frac{n_i(h)}{n_{i,crit}}\right)^2\right) \tag{1}$$

as an NFD-type approximation function to regional production, where $v_{i,f} \in \mathbb{R}^+$ is average speed (km/h) for region i under free-flow conditions, $n_i(h)$ is vehicle count for region i at step h and $n_{i,crit}$ is the vehicle count critical value for region i. The flow from region i to j, $i,j \in \mathcal{N}, (i,j) \in \mathcal{A}$ is derived from the NFD and can be separated in supply $P_j(h)$ and demand $Z_{i,j}(h)$ for step h. Supply and demand can be expressed through (1). Concretely, when vehicle count $n_i(h)$ falls below critical value $n_{i,crit}$, supply $P_j(h)$ becomes equal to regional capacity production $Q_{j,crit}$. In any other case, $P_j(h)$ follows a scaled-down NFD curve. When vehicle count $n_i(h)$ becomes greater than $n_{i,crit}$, demand $Z_{i,j}(h)$ from region i to j decreases. Thus, any restriction imposed on the outflow, caused by intraregional travel demand, is implicitly taken into account. Demand $Z_{i,j}(h)$ is further restricted by the interregional boundary capacity, which leads to effective demand

$$\tilde{Z}_{i,j}(h) = \min\left\{Z_{i,j}(h), b_{i,j}\right\}, \tag{2}$$

from region i to j at step h. For our multi-class extension, effective demand can be further decomposed into $\tilde{Z}^k_{i,j,\alpha,\omega}(h)$, representing k-class, α-origin, ω-destination specific demands from region i to j at step h. Once all incoming demands to j are aggregated to total demand

$$Z_j(h) = \sum_{i\in\mathcal{N},(i,j)\in\mathcal{A}} \tilde{Z}_{i,j}(h), \tag{3}$$

the flow proportion entering j is

$$\epsilon_j(h) = \min_{j\in\mathcal{N},(i,j)\in\mathcal{A}} \left\{\frac{P_j(h)}{Z_j(h)}, 1\right\} \tag{4}$$

Subsequently, flow proportion

$$\chi_i(N) = \min_{j\in\mathcal{N},(i,j)\in\mathcal{A}} \left\{\epsilon_j(h)\right\} \tag{5}$$

will be the same for all demands $Z_{i,j}(h)$, under the assumption that interregional traffic transition is restricted, due to congestion caused by intraregional travel demand, in addition to spillback along the boundaries. If the supply restricts the flow, region j receives a proportion of the flow, analogous to the demands converging to j. Outflow $q_{i,j}(h)$, in effect the minimum of supply $P_j(h)$ and demand $Z_{i,j}(h)$, is assumed constant between time steps, and can be decomposed into $q^k_{i,j,\alpha,\omega}(h)$, a k-class, α-origin, ω-destination specific outgoing flow. Finally, we derive the state equations for our dynamic model:

State equations:

$$n_i(h+1) = \sum_{\omega \in \mathcal{N}_t} \sum_{\alpha \in \mathcal{N}_s} \sum_{k \in \mathcal{K}} n^k_{i,\alpha,\omega}(h+1),$$

with

$$n^k_{i,\alpha,\omega}(h+1) = n^k_{i,\alpha,\omega}(h) + \frac{T_{sample}}{\sum_{l \in \mathcal{L}_i} \lambda_l \Lambda_l} \left(\sum_{j \in \mathcal{N}, (i,j) \in \mathcal{A}} q^k_{j,i,\alpha,\omega}(h) - \sum_{j \in \mathcal{N}, (i,j) \in \mathcal{A}} q^k_{i,j,\alpha,\omega}(h) \right)$$

where λ_l, Λ_l, the number of lanes and length of link $l \in \mathcal{L}_i$ respectively;

Control variables:

$\beta^{p,k}_{i,j,\alpha,\omega}(h)$: p-path, k-class, α-origin, ω-destination specific branching rates from region i to j, at step h, where $p \in \mathcal{P}_{\alpha,\omega}$

III. Region-based Routing

We will present the routing methods associated with each traveler class mentioned earlier, in a reverse order. Starting from 3^{rd} class travelers employing conventional vehicles without any RGIS, continuing with 2^{nd} class that make use of conventional vehicles equipped with RGIS and finishing with 1^{st} class, which employs autonomous vehicles.

A. Assumptions

Before presenting the routing methods, certain assumptions need to be made:

- Each traveler belonging to 1^{st} and 2^{nd} class is assumed to own a navigation device. They are able to receive route advice as announcements from the routing information provider at the beginning of each trip.
- Pre-trip route advice is available for dissemination at each sample interval.
- Once a pre-trip choice from the set of available routes is provided at the Origin, travelers are expected to not make any other route choices throughout their trips.
- For all OD-pairs, public transit is available with infinite capacity and constant travel time.

B. Routing for 3^{rd} class travelers

In the literature, multinomial probit and multinomial logit route choice models have been used to represent self-interested driver behavior, by deriving Dynamic Stochastic User Equilibria (DSUE), both for link-based urban traffic networks [31]–[33] and regional traffic networks [18], [20], [34]. While multinomial logit route choice models have a closed-form expression of the probability approximating DSUE, they lack the ability to account for path overlap, or perception variance with respect to paths of varying lengths. Multinomial probit choice models account for both, however they have no closed-form expression, requiring heuristic techniques such as the Method of Successive Averages (MSA) to arrive at a DSUE. For a more realistic, yet less computationally expensive route choice, we introduce a region-based extension to the Hybrid Route Choice (HRC) model of Xu et al. [35]. This model has a closed-form expression of the probability approximating DSUE, but can also account for path overlap and perception variance with respect to paths of varying lengths. We assign a probability to each alternate path μ with travel time TT_μ from a set of κ shortest paths, as follows:

$$P(\mu|\kappa) = \frac{e^{-\theta TT_\mu - \gamma ln TT_\mu}}{\sum_{\nu \in \kappa} e^{-\theta TT_\nu - \gamma ln TT_\nu}} \tag{6}$$

where θ and γ are the scale and shape parameter respectively. In our case study, $\theta = 0.16$ and $\gamma = 2.1$, to account for the travel time units used therein. The hybrid route choice model is extended to take into consideration the fact that travelers choose to travel by public transit. The κ-shortest path set for every regional OD-pair is updated according to $v_i(h), \forall i \in \mathcal{N}$ at current step h. All OD-pair paths used in public transit are considered to have constant speed $v_{i,PT} = 0.5 v_{i,f}$ and the public transit travel times are calculated accordingly.

C. Routing for 2^{nd} class travelers

For the conventional connected vehicles, equipped with RGIS, a strategic learning-based algorithm employing Modified Regret Matching (MRM) is considered. This approach uses a simple compliance model that tests for different compliance rates set before each simulation and is meant to describe the behavior of 2^{nd} class travelers. We employ the concept of repeated games, with Origins as players, competing for a single Destination. In our case, it is assumed that the bipartite graph of Origins and Destinations is complete, i.e. all Origins can reach all Destination regions. This entails the simultaneous play of a set of repeated games and in each game all regions that belong to $\mathcal{N}_s$ compete for one specific Destination region $\omega \in \mathcal{N}_t$. Player actions can be described as probability distributions over the κ-shortest paths available for each region $\alpha \in \mathcal{N}_s$. For each $\omega \in \mathcal{N}_t$, at each repeated game iteration, each $\alpha \in N_s$ selects a set of routes from α to ω, based on experienced average past regrets.
In the first step of this routing method, Yen's algorithm [36] is used to find the sets of κ-shortest paths.
In the second step of this routing method, data preprocessing takes place, for increased computational efficiency. During this process, which allows for the public transit diversion component to take effect, the use of every region i where at step h, $n_i(h) > n_{i,crit}, i \in \mathcal{N}, h \in \mathcal{H}$, is precluded from all κ-shortest path set calculations at time step h. If the resulting path set is empty, the public transit diversion component is activated. In the final step, Modified Regret Matching is used to derive the probability distributions for each set of κ-shortest paths. Concretely, for Destination $\omega \in \mathcal{N}_t$, we define

the average Modified Regret of player α for $y \in P_{\alpha,\omega}$ to $z \in P_{\alpha,\omega}$ at step h as

$$\hat{M}_{\alpha}^{h}(y,z) = max\left\{\frac{1}{h}\left[\sum_{\eta\leq h:p_{\alpha}^{\eta}=z}\frac{\sigma_{\alpha}^{\eta}(y)}{\sigma_{\alpha}^{\eta}(z)}U_{\alpha}^{\eta}(p_{\alpha}^{\eta}) - \sum_{\eta\leq h:p_{\alpha}^{\eta}=y}U_{i}^{\eta}(p_{\alpha}^{\eta})\right],0\right\} \quad (7)$$

with $\sum_{y=1}^{p_\alpha}\sigma_{\alpha}^{\eta}(y) = 1$, where $\sigma_{\alpha}^{\eta}(y)$ denotes the play probability for player $\alpha \in \mathcal{N}_s$, $U_{\alpha}^{\eta}(p_{\alpha}^{\eta})$ the utility received by player α for selecting action p_{α}^{η} and η all plays up to h. The player calculates the Modified Regret and subsequently updates the probability accordingly. If the player selects action y at step h, the probability of selecting action z at step $h+1$ is approximately proportional to the average Modified Regret from y to z. The play probabilities of player α at step $h+1$ are assigned as follows

$$\sigma_{\alpha}^{h+1}(z) = \left(1-\frac{\delta}{h^{\gamma}}\right)min\left\{\frac{\hat{M}_{\alpha}^{h}(y,z)}{\mu},\frac{1}{|P_{\alpha,\omega}|-1}\right\} + \frac{\delta}{h^{\gamma}p_i},\ z\neq y, z\in P_{\alpha,\omega} \quad (8)$$

and

$$\sigma_{\alpha}^{h+1}(y) = 1 - \sum_{w\in P_{\alpha,\omega}:w\neq x}\sigma_{\alpha}^{h+1}(w) \quad (9)$$

where $\delta \in [0,1]$, $\gamma < 0.25$ and inertia parameter μ large enough to guarantee that $\sigma_{\alpha}^{h+1}(y) > 0$.

D. Routing for 1^{st} class travelers

For the predictive routing method associated with 1^{st} class travelers, we have selected to use Incremental Route Guidance (IRG), a simulation-based predictive approach to route guidance, similar to the predictive routing method introduced in [20]. This method consists of 2 steps, the planning step and the shortest path computation and assignment step. During the planning step, regional travel demand fractions are introduced to the network and regional traffic dynamics for demand fractions already present at the network are simulated. The simulation is advanced until all vehicles complete their trips. Virtual vehicles assumed to employ hybrid routing are also generated. Virtual vehicle trip generation allows for more accurate travel time estimation and also discourages the frequent use of Origin regions during path set computation. Subsequently, for the shortest path set computation and assignment step, we employ a time-expanded network representation $\bar{G} = (\bar{\mathcal{N}}, \bar{\mathcal{A}})$, with $\bar{\mathcal{N}} = \left\{i^h | i \in \mathcal{N}, h \in \mathcal{H}\right\}$ a set of time-expanded regions, $\bar{\mathcal{A}} = \{(i^h, j^{h'}) | (i,j) \in \mathcal{A}, h + w_{i,j}^h = h', h_0 \leq h \leq h' \leq h_0 + \Gamma g\}$ a set of interregional time-dependent transitions along the set of boundaries $\mathcal{A}$. Weight $w_{i,j}^h \in \mathcal{H}$ is assigned, at time h, for time-expanded regions $i^h, j^{h'} \in \bar{\mathcal{N}}, (i^h, j^{h'}) \in \bar{\mathcal{A}}$, as the time necessary for the departing vehicle to traverse region i and enter region j. For each $\alpha \in \mathcal{N}_s$, the discrete time step $h = h_0 + \nu g$, $\nu \in \mathbb{N}^+$ represents vehicle departure time at time-expanded Origin α^h. For each $\omega \in \mathcal{N}_t$, the arrival time depends on prevailing traffic and the route selected from the κ-shortest paths, thus cannot be set in advance. So Destination $\omega^{\emptyset}$ is introduced, to represent trip completion with undetermined arrival time $\emptyset$. The resulting graph $\bar{G}$ contains the set of all eligible paths $\bar{\mathcal{P}}_{\alpha^h,\omega^{\emptyset}}$ from α^h to $\omega^{\emptyset}, \forall \alpha \in \mathcal{N}_s, \omega \in \mathcal{N}_t$. If $\tilde{H} = H - h, \Theta = [h, ..., h+\tilde{H}]$, if $i^{\theta} | n_i(\theta) > n_{i,crit}, \forall i^{\theta} \in p^{\theta} \in \bar{\mathcal{P}}_{\alpha^{\theta},\omega^{\emptyset}}, \theta \in \Theta$, the set of eligible paths $\bar{\mathcal{P}}_{\alpha^h,\omega^{\emptyset}}$ contains only regions $i | n_i(\theta) > n_{i,crit}, i \in \mathcal{N}$. If the path set is empty, the public transit diversion component comes into effect.

IV. Experiments

A honeycomb network is considered for implementation of the McNTM. The network consists of 16 hexagonal regions, with a radius of 2.69km^2 and an area of 25km^2 for each region, as shown in Fig. 1

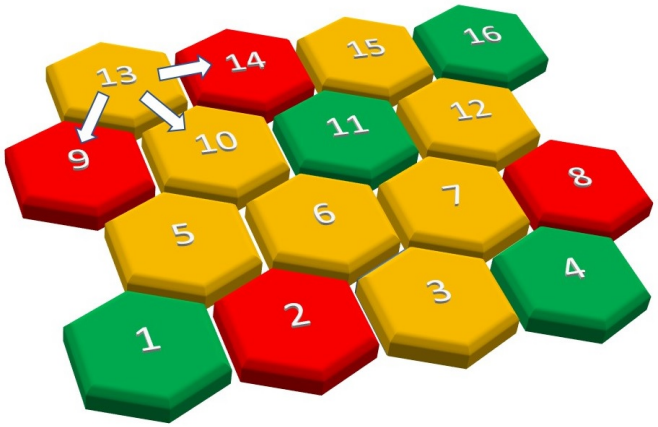

Fig. 1. Layout of the honeycomb regional network, where green and red hexagons denote Origins and Destinations, respectively.

The homogeneous regions are each described by an NFD with critical accumulation $n_{i,crit}$ = 25veh/km, region network length $\sum_{l\in\mathcal{L}_i}\lambda_l\Lambda_l$ = 16.14 km and free flow speed $v_{i,f}$ = 45km/h, $\forall i \in \mathcal{N}$. Capacity along the boundaries is $b_{i,j}$ = 2000veh/h/lane, $\forall i,j \in \mathcal{N}, (i,j) \in \mathcal{A}$. For each region i, all regions j such that $(i,j) \in \mathcal{A}$ are defined as the ones that are adjacent to region i. The simulation horizon H=2h30min or 9000s. The sample time T_{sample}=10s.

A. Performance Metrics

Several performance metrics are now defined, by which an effort will be made to compare the effects of each region-based routing method on the regional network performance:

- $\mathcal{C}_{\text{PTD}}$, public transit diversion, travel demand proportion diverted to Public Transit (%)

- $\mathcal{C}_{\text{ITR}}$, Incomplete Trips Rate, i.e., travel demand proportion with unfinished trips at simulation end (%)
- $\mathcal{C}_{\text{ATT}}$, Average Travel Time for each traveler on the regional urban network (s)
- $\mathcal{C}_{\text{TVT}} = T_{sample} \sum_{h=1}^{H} \sum_{i \in \mathcal{N}} \left(\sum_{l \in \mathcal{L}_i} \lambda_l \Lambda_l n_i(h) \right)$, Total Vehicle Travel time for all regions ($veh \cdot s$)
- $\mathcal{C}_{\text{v}^2} = \sum_{h=1}^{H} \sum_{i,j \in \mathcal{N}} \left(v_i(n_i(h)) - v_j(n_j(h)) \right)^2$ Sum of Squares of average regional speed variabilities for all regions (km^2/h^2), which measures the homogeneity of traffic load distribution

$\mathcal{C}_{\text{PTD}}$ represents the number of potential travelers unable to utilize the urban network, as a fraction of the number of vehicle requests from all regional OD-pairs. Since the speed selected for public transit is lower than the average speed corresponding to the critical accumulation value, $\mathcal{C}_{\text{PTD}}$ implicitly shows the aggregate cost of low network resource utilization due to oversaturated traffic conditions. The Incomplete Trips Rate $\mathcal{C}_{\text{ITR}}$ implicitly showcases the network throughput performance. $\mathcal{C}_{\text{ATT}}$ is calculated as the weighted average of total travel time for all vehicles and provides an easily quantifiable measure of individual traveler benefits. $\mathcal{C}_{\text{TVT}}$ can be considered as a measure of overall network performance. $\mathcal{C}_{\text{v}^2}$ indirectly shows how congestion can exceed capacity in some regions, while other regions remain relatively empty.

B. Market Penetration Scheme

As mentioned in the introduction, we make use of scenario 2 (S2) from [3] to construct a market penetration scheme that forecasts moderate autonomous technology adoption over a span of 25 years, starting from year 2020. In table I, the different market penetration rates (MPR) for each traveler class are presented.

TABLE I
S2

MPRs for each Traveler Class			
Year	**1^{st}(MPR1)**	**2^{nd}(MPR2)**	**3^{rd}(MPR3)**
2020	3.0%	15.0%	82.0%
2025	10.2%	25.0%	64.8%
2030	19.0%	27.1%	53.9%
2035	28.7%	28.9%	42.4%
2040	37.9%	23.5%	38.6%
2045	43.8%	39.7%	16.5%

C. Results

The performance results for each market penetration rate combination, assuming that the 2^{nd} traveler class remains compliant, can be seen on table II. We can observe that, 1^{st} class travelers wil have, throughout the years, the lowest $\mathcal{C}_{ATT}$ and the highest $\mathcal{C}_{PTD}$. Obviously, it is to be expected, that these two metrics have an inverse relationship. The more travelers encouraged to use Public Transit, the fewer there are to cause congestion on the urban traffic network. Another important metric, $\mathcal{C}_{ITR}$, is consistently kept below 5%, for both 1^{st} and 2^{nd} traveler classes, while it can exceed 20% for the 3^{rd} traveler class. It should also be noted that the respective market penetration rate plays a significant part in the individual performance metric results. While MPR3 remains over 40%, with MPR1 and MPR2 values not exceeding 30%, $\mathcal{C}_{ATT}$ for 3^{rd} class travelers keeps performing the worst, however, this changes for the Year 2040, where MPR1 and MPR3 exceed 35%, with $\mathcal{C}_{ITR}$ for 3^{rd} class travelers increasing, after it had been consistently decreasing before. HRC, employed by 3^{rd} traveler class, under-performs in all performance metrics except for $\mathcal{C}_{PTD}$. This can be attributed to the public transit diversion component stochasticity for HRC. Assuming that all metrics are of equal importance, we can see a slight, yet not insignificant, gain in overall performance for the case where 1^{st} and 2^{nd} class travelers are present in the system, ranging from 0.78% - 23.43% throughout the span of 25 years, over the case where the network is comprised solely of 3^{rd} class travelers, i.e. with MPR3=100%. This means that IRG, in combination with MRM, employed by the 1^{st} and 2^{nd} class respectively, not only benefit overall network performance, but with their respective MPR1 and MPR2 exceeding certain thresholds, can affect a positive influence to the individual performance of other traveler classes, as can be observed by comparing the results for Years 2020-2045.

TABLE II
COMPARISON OF PERFORMANCE METRICS FOR EACH TRAVELER CLASS IN MIXED APPLICATION OF IRG, MRM AND HRC FOR $S2$

Scenario (S2)					
	Year 2020				
Metrics	$\mathcal{C}_{TVT}$	$\mathcal{C}_{v2}$	$\mathcal{C}_{PTD}$	$\mathcal{C}_{ITR}$	$\mathcal{C}_{ATT}$
IRG	4.259e+08	1.583e+07	70.91	0.19	2186.6
MRM	4.259e+08	1.583e+07	68.97	0.97	2768.3
HRC	4.259e+08	1.583e+07	35.15	20.39	3254.9
	Year 2025				
Metrics	$\mathcal{C}_{TVT}$	$\mathcal{C}_{v2}$	$\mathcal{C}_{PTD}$	$\mathcal{C}_{ITR}$	$\mathcal{C}_{ATT}$
IRG	3.765e+08	1.478e+07	73.98	0.65	2302.6
MRM	3.765e+08	1.478e+07	65.17	1.96	2944.3
HRC	3.765e+08	1.478e+07	34.50	14.71	3190.8
	Year 2030				
Metrics	$\mathcal{C}_{TVT}$	$\mathcal{C}_{v2}$	$\mathcal{C}_{PTD}$	$\mathcal{C}_{ITR}$	$\mathcal{C}_{ATT}$
IRG	3.677e+08	1.354e+07	70.95	1.74	2576.0
MRM	3.677e+08	1.354e+07	61.41	2.62	3015.8
HRC	3.677e+08	1.354e+07	29.49	11.35	3064.2
	Year 2035				
Metrics	$\mathcal{C}_{TVT}$	$\mathcal{C}_{v2}$	$\mathcal{C}_{PTD}$	$\mathcal{C}_{ITR}$	$\mathcal{C}_{ATT}$
IRG	3.254e+08	1.056e+07	69.69	2.17	2373.7
MRM	3.254e+08	1.056e+07	52.31	2.66	2609.8
HRC	3.254e+08	1.056e+07	19.01	6.48	2535.4
	Year 2040				
Metrics	$\mathcal{C}_{TVT}$	$\mathcal{C}_{v2}$	$\mathcal{C}_{PTD}$	$\mathcal{C}_{ITR}$	$\mathcal{C}_{ATT}$
IRG	3.332e+08	9.943e+06	62.12	3.56	2263.7
MRM	3.332e+08	9.943e+06	50.21	2.29	2570.6
HRC	3.332e+08	8.304e+06	15.58	7.44	2610.8
	Year 2045				
Metrics	$\mathcal{C}_{TVT}$	$\mathcal{C}_{v2}$	$\mathcal{C}_{PTD}$	$\mathcal{C}_{ITR}$	$\mathcal{C}_{ATT}$
IRG	2.836e+08	8.304e+06	62.22	2.65	2156.4
MRM	2.836e+08	8.304e+06	40.08	3.10	2386.3
HRC	2.836e+08	8.304e+06	11.89	2.14	2316.4

V. Conclusions and Future Work

In this work, we have introduced a simulation modeling framework that can accommodate multiple classes of travelers and integrates several distinct features. These features include a public transit diversion component, as well as routing methods, which are associated with different traveler classes. We choose to associate autonomous vehicles with the 1^{st} class of travelers which employs predictive routing and are expected to be fully compliant. We associate conventional connected vehicles, equipped with non-predictive RGIS (Route Guidance and Information Systems), with the 2^{nd} traveler class. Travelers that belong to this class, have the option to ignore the routing information prescribed to them. We associate all unequipped conventional vehicles with the 3^{rd} traveler class. We have observed that the gain in overall performance for the case where 1^{st} and 2^{nd} class travelers are present in the system, ranges from 0.78% - 23.43%. Region-based routing methods employed by the 1^{st} (IRG) and 2^{nd} (MRM) class respectively, not only benefit overall network performance, but with their respective market penetration rates exceeding certain thresholds, can positively influence the individual performance of other traveler classes.

These results provide incentive for further investigation of applications for our simulation modeling framework. In our next step, we aim to implement the bi-directional model as part of the 2^{nd} class of travelers, as well as add further sophistication to our public transit model, taking into consideration the delay incurred from transferring to public transit. We are also looking into alternative autonomous vehicle technology adoption scenarios, where regulations are enforced and the market penetration rate of autonomous vehicles is expected to be higher. Last but not least, we aim to use our model to investigate the effects of ridesharing in conjunction with public transit diversion and varying degrees of compliance, on individual traveler class as well as overall network performance.

References

[1] A. Augustine and M. Nava, "Auto dealerships: Destined for disruption," 2016.

[2] A. Skabardonis, P. Varaiya, and K. Petty, "Measuring recurrent and nonrecurrent traffic congestion," *Transportation Research Record: Journal of the Transportation Research Board*, no. 1856, pp. 118–124, 2003.

[3] P. Bansal and K. M. Kockelman, "Forecasting americans long-term adoption of connected and autonomous vehicle technologies," *Transportation Research Part A: Policy and Practice*, vol. 95, pp. 49–63, 2017.

[4] N. Geroliminis and J. Sun, "Properties of a well-defined macroscopic fundamental diagram for urban traffic," *Transportation Research Part B: Methodological*, vol. 45, no. 3, pp. 605–617, 2011.

[5] A. Mazloumian, N. Geroliminis, and D. Helbing, "The spatial variability of vehicle densities as determinant of urban network capacity," *Philosophical Transactions of the Royal Society A: Mathematical, Physical and Engineering Sciences*, vol. 368, no. 1928, pp. 4627–4647, 2010.

[6] C. F. Daganzo, V. V. Gayah, and E. J. Gonzales, "Macroscopic relations of urban traffic variables: Bifurcations, multivaluedness and instability," *Transportation Research Part B: Methodological*, vol. 45, no. 1, pp. 278–288, 2011.

[7] K. Aboudolas and N. Geroliminis, "Perimeter and boundary flow control in multi-reservoir heterogeneous networks," *Transportation Research Part B: Methodological*, vol. 55, pp. 265–281, 2013.

[8] M. Hajiahmadi, J. Haddad, B. De Schutter, and N. Geroliminis, "Optimal hybrid macroscopic traffic control for urban regions: Perimeter and switching signal plans controllers," in *Control Conference (ECC), 2013 European*. IEEE, 2013, pp. 3500–3505.

[9] J. Haddad, M. Ramezani, and N. Geroliminis, "Cooperative traffic control of a mixed network with two urban regions and a freeway," *Transportation Research Part B: Methodological*, vol. 54, pp. 17–36, 2013.

[10] M. Keyvan-Ekbatani, M. Papageorgiou, and I. Papamichail, "Urban congestion gating control based on reduced operational network fundamental diagrams," *Transportation Research Part C: Emerging Technologies*, vol. 33, pp. 74–87, 2013.

[11] N. Geroliminis and D. M. Levinson, "Cordon pricing consistent with the physics of overcrowding," in *Transportation and Traffic Theory 2009: Golden Jubilee*. Springer, 2009, pp. 219–240.

[12] N. Zheng, R. A. Waraich, K. W. Axhausen, and N. Geroliminis, "A dynamic cordon pricing scheme combining the macroscopic fundamental diagram and an agent-based traffic model," *Transportation Research Part A: Policy and Practice*, vol. 46, no. 8, pp. 1291–1303, 2012.

[13] M. Simoni, A. Pel, R. Waraich, and S. Hoogendoorn, "Marginal cost congestion pricing based on the network fundamental diagram," *Transportation Research Part C: Emerging Technologies*, vol. 56, pp. 221–238, 2015.

[14] S. Zhong, M. Bushell, and W. Deng, "A reliability-based stochastic system optimum congestion pricing model under atis with endogenous market penetration and compliance rate," in *Transportation Research Board 91st Annual Meeting*, no. 12-1001, 2012.

[15] N. Zheng, G. Rérat, and N. Geroliminis, "Time-dependent area-based pricing for multimodal systems with heterogeneous users in an agent-based environment," *Transportation Research Part C: Emerging Technologies*, vol. 62, pp. 133–148, 2016.

[16] M. Hajiahmadi, V. L. Knoop, B. De Schutter, and H. Hellendoorn, "Optimal dynamic route guidance: A model predictive approach using the macroscopic fundamental diagram," in *Intelligent Transportation Systems-(ITSC), 2013 16th International IEEE Conference on*. IEEE, 2013, pp. 1022–1028.

[17] V. Knoop, S. Hoogendoorn, and J. W. Van Lint, "Routing strategies based on macroscopic fundamental diagram," *Transportation Research Record: Journal of the Transportation Research Board*, vol. 2315, no. 1, pp. 1–10, 2012.

[18] M. Yildirimoglu, M. Ramezani, and N. Geroliminis, "Equilibrium analysis and route guidance in large-scale networks with mfd dynamics," *Transportation Research Part C: Emerging Technologies*, 2015.

[19] A. F. Lentzakis, S. I. Ware, and R. Su, "Region-based dynamic forecast routing for autonomous vehicles," in *Intelligent Transportation Systems (ITSC), 2016 IEEE 19th International Conference on*. IEEE, 2016, pp. 1464–1469.

[20] A. F. Lentzakis, S. I. Ware, R. Su, and C. Wen, "Region-based prescriptive route guidance for travelers of multiple classes," *Transportation Research Part C: Emerging Technologies*, vol. 87, pp. 138–158, 2018.

[21] D. de Jong, V. L. Knoop, and S. P. Hoogendoorn, "The effect of signal settings on the macroscopic fundamental diagram and its applicability in traffic signal driven perimeter control strategies."

[22] V. V. Gayah, X. S. Gao, and A. S. Nagle, "On the impacts of locally adaptive signal control on urban network stability and the macroscopic fundamental diagram," *Transportation Research Part B: Methodological*, vol. 70, pp. 255–268, 2014.

[23] J. Laval, "The effect of signal timing and network irregularities in the macroscopic fundamental diagram," in *Proceedings of the summer meeting of the TFTC TRB committee*, 2010, p. 5.

[24] L. Leclercq, N. Geroliminis *et al.*, "Estimating mfds in simple networks with route choice," *Transportation Research Part B: Methodological*, vol. 57, no. C, pp. 468–484, 2013.

[25] Y. Ji and N. Geroliminis, "On the spatial partitioning of urban transportation networks," *Transportation Research Part B: Methodological*, vol. 46, no. 10, pp. 1639–1656, 2012.

[26] A. F. Lentzakis, R. Su, and C. Wen, "Time-dependent partitioning of urban traffic network into homogeneous regions," in *Control Automation Robotics & Vision (ICARCV), 2014 13th International Conference on*. IEEE, 2014, pp. 535–540.

[27] M. Saeedmanesh and N. Geroliminis, "Dynamic clustering and propagation of congestion in heterogeneously congested urban

traffic networks," *Transportation Research Procedia*, vol. 23, pp. 962–979, 2017.
[28] S. Feigon and C. Murphy, *Shared mobility and the transformation of public transit*, 2016, no. Project J-11, Task 21.
[29] B. Preston, "Elaine chao says deregulation should smooth the way for autonomous vehicles," 2018, online; accessed 30-April-2018. [Online]. Available: http://www.thedrive.com/tech/18123/elaine-chao-says-deregulation-should-smooth-the-way-for-autonomous-vehicles
[30] V. L. Knoop and S. P. Hoogendoorn, "Simulation model for traffic using network fundamental diagrams," in *Traffic and Granular Flow'13*. Springer, 2015, pp. 379–384.
[31] Y. Sheffi, "Urban transportation network," *Equilibrium analysis with mathematical programming methods, Prentice Hall*, 1985.
[32] Q. Meng, D.-H. Lee, R. L. Cheu, and H. Yang, "Logit-based stochastic user equilibrium problem for entry-exit toll schemes," *Journal of transportation engineering*, vol. 130, no. 6, pp. 805–813, 2004.
[33] Q. Meng and H. L. Khoo, "A computational model for the probit-based dynamic stochastic user optimal traffic assignment problem," *Journal of Advanced Transportation*, vol. 46, no. 1, pp. 80–94, 2012.
[34] M. Yildirimoglu and N. Geroliminis, "Approximating dynamic equilibrium conditions with macroscopic fundamental diagrams," *Transportation Research Part B: Methodological*, vol. 70, pp. 186–200, 2014.
[35] X. Xu, A. Chen, S. Kitthamkesorn, H. Yang, and H. K. Lo, "Modeling absolute and relative cost differences in stochastic user equilibrium problem," *Transportation Research Part B: Methodological*, vol. 81, pp. 686–703, 2015.
[36] J. Y. Yen, "Finding the k shortest loopless paths in a network," *management Science*, vol. 17, no. 11, pp. 712–716, 1971.